Proceedings of the 6th International Conference on Gas Hydrates (ICGH 2008),
Vancouver, British Columbia, CANADA, July 6-10, 2008.

MOLECULAR SIMULATIONS OF GAS HYDRATES: PREDICTIONS OF STRUCTURE, STABILITY, AND VIBRATIONAL BEHAVIOR

Jeffery A. Greathouse* and Randall T. Cygan
Geochemistry Department
Sandia National Laboratories
Albuquerque, New Mexico, 87185-0754
USA

ABSTRACT

Recent advances in computational power and simulation methods have led to the application of molecular modeling to larger and more complex gas hydrate systems. In the area of classical atomistic simulations, including Monte Carlo methods and molecular dynamics, nanometer (and larger) length scales, and nanosecond time scales are now accessible. This paper focuses on molecular dynamics simulations of structure I and structure II gas hydrates, using a general classical force field (CVFF) to treat guest-host interaction parameters. Molecular flexibility (bond stretch, angle bend, torsion) are included in the simulations, so computed molecular geometries and vibrational modes can be readily compared with experiment. Applications include methane hydrates for force field validation as well as hydrochlorofluorocarbon (HCFC) hydrates for potential use in water desalination. Thermal expansion results for sI methane hydrate are in good agreement with experiment. Vibrational power spectra show a difference in C-H stretch frequencies for methane molecules in large and small cages. Also, simulated vibrational frequencies of pure methane gas are more closely matched by methane molecules in large cages. We also consider a sII hydrate in which the large cages are occupied by 1,1-dichloro-1-fluoroethane (R141b). R141b hydrate exhibits mild forming conditions (265 K), indicating that HCFC hydrates may have a potential use in water desalination. Despite evidence of hydrogen bonding between R141b and water, the guest molecule rotates freely within the large cage. The 1,2-dichloro isomer of R141b forms a sII hydrate at much lower temperatures (150 K) due to its larger molecular diameter. Electron density plots from quantum calculations show significant electronic overlap between the isomer and water molecules, while no overlap exists for R141b.

Keywords: molecular dynamics, density functional theory, stability, vibrational spectroscopy

NOMENCLATURE

N Number of particles
P Pressure [bar]
T Temperature [K]
V Volume [Å^3]

INTRODUCTION

Computational methods have been increasingly used to study molecular and thermodynamic properties of gas hydrates [1-10]. Most of the attention has focused on methane hydrates, and the goal of these projects has been to validate the published experimental data on thermodynamics of hydrate formation [2-10]. Most molecular simulation studies to date have focused on simple energy force fields, treating water molecules as rigid bodies and methane molecules as spherical particles. Such a simple approach has been used to compare the thermodynamics of cage occupancies with predictions from statistical thermodynamics [2, 7, 10].

The use of relatively simple force fields may be sufficient for studies of phase behavior or thermodynamic properties, but not for molecular detail such as vibrational modes. Molecular

* Corresponding author: Phone: +1 505 284 4895 Fax +1 505 844 7354 E-mail: jagreat@sandia.gov

dynamics methods can be used to provide vibrational frequencies in the form of a power spectrum [11]. Provided that molecular flexibility in the form of bond stretching and angle bending terms are included in the force field energy expression, dynamics trajectories can be analyzed and spectra can be calculated.

In this study, we use molecular dynamics simulation to examine the molecular structure, thermal stability, and vibrational spectra for a sI hydrate (methane) as well as sII hydrates using dichlorofluoroethane guests. A general force field for organics (Consistent Valence Force Field, CVFF) [12] was used with no modification of parameters. The advantage of a general force field is its transferability to new hydrate systems without the need to derive new water-guest interaction parameters. Additionally, our simulation results are validated by comparisons with electronic structure calculations using density functional theory (DFT).

METHODS

The computational methods approach used in this study follows from previous work [13, 14] and will only be summarized here. Initial atomic coordinates and lattice parameters were taken from experimental crystal structures [15, 16]. In the case of methane hydrate, one molecule was placed in each cage of the sI hydrate structure. Guest molecules for the sII hydrates consisted of either 1,1-dichloro-1-fluoroethane (R141b) or its isomer, 1,2-dichloro-1-fluoroethane. One guest molecule was placed in each large cage, while the small cages were empty.

DFT Methods

Electronic structure calculations were performed using the density functional code DMol^3 [17, 18] on cluster models of the structure II large ($5^{12}6^4$) and small (5^{12}) hydrate cages with the dichlorofluoroethane guests. Vibrational spectra for the cluster models the were derived using normal mode analysis [19].

Classical Molecular Dynamics

Classical simulations were performed with the Open Force Field module of Cerius^2 (Accelrys, Inc.). Simulations were performed in both the constant pressure (NPT) and constant volume (NVT) ensembles. Vibrational power spectra were obtained by taking the Fourier transform of the velocity autocorrelation functions (VACFs) for each atom type [11].

RESULTS

Methane Hydrate

Structural information obtained from the NPT simulations were compared with available neutron diffraction results [20, 21]. Figure 1 shows the simulated thermal expansion trend of the lattice parameters from 0 K to 300 K. The data point at 0 K was obtained by performing an energy minimization using the Cerius^2 OFF Minimizer while allowing the cell volume to vary. The simulation results are in qualitative agreement with the neutron diffraction data of CD_4 hydrates [20], but the lattice parameters are shifted to smaller values by approximately 0.15 Å at each temperature. The fact that the experimental lattice parameters for CD_4 and CH_4 hydrates at 100 K disagree by 0.08 Å suggests that there is some variability in those results as well. Additionally, the CD_4 hydrate patterns also contained signals for hexagonal ice Ih and solid N_2 [20]. Overall we find excellent agreement between the simulated and experimental lattice constants over the temperature range 60 K - 200 K.

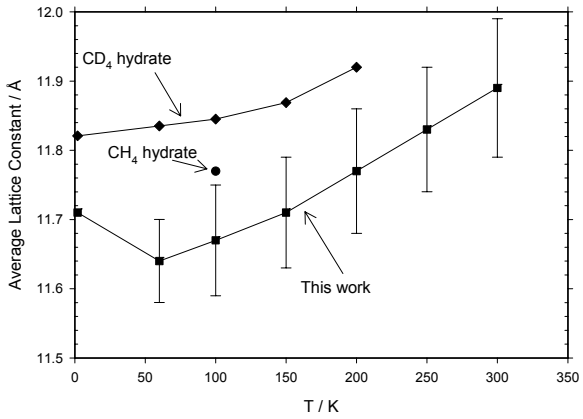

Figure 1 Average lattice parameters for methane hydrate as a function of temperature. Experimental values (errors less than 0.01 Å) obtained from neutron diffraction are also shown for CD_4 hydrate [20] and CH_4 hydrate [21]. Reprinted with permission from ref. 13. Copyright 2006 American Chemical Society.

Separate NVT simulations were performed to obtain atomic power spectra of methane molecules in both the gas (300 bar) and hydrate phases. Power spectra of the methane hydrogen atoms at 273 K are shown in Figure 2. The four vibrational

modes of methane are easily seen, but the assignment of normal modes required a separate calculation of only C atoms. The librational motion of methane molecules in small cages occurs at a higher frequency (102 cm^{-1}) than methane molecules in the large cages (61 cm^{-1}) due to the reduced free volume in the small cage.

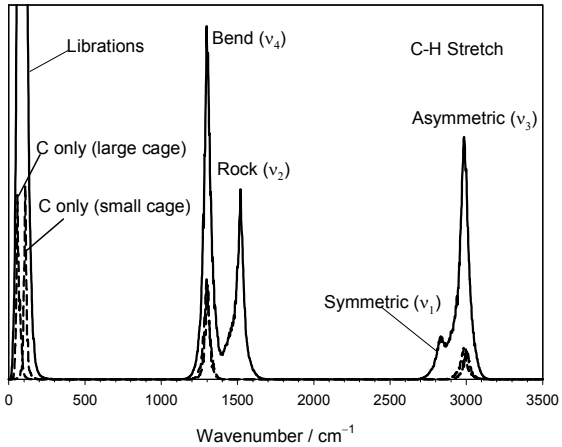

Figure 2 Simulated power spectra of methane molecules in methane hydrate. The solid line represents methane H atoms, and the dashed lines represent methane C atoms in large and small cages. The C atom peaks at 1300 cm^{-1} and 3000 cm^{-1} were multiplied by a factor of 50 for ease of viewing. Contributions from water molecules are not shown for clarity. Reprinted with permission from ref. 13. Copyright 2006 American Chemical Society.

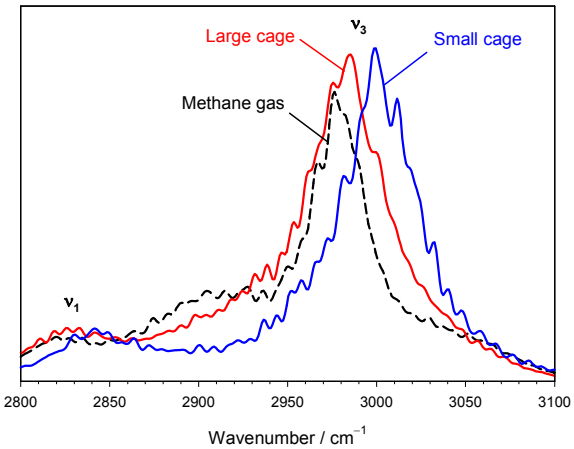

Figure 3 Simulated power spectra of methane H atoms in hydrate (solid lines) and gas (dashed line) phases, focusing on the C-H stretch region. Reprinted with permission from ref. 13. Copyright 2006 American Chemical Society.

The C-H stretching modes can also be used to distinguish between methane in small and large cages, as seen in Figure 3. Peaks for the small and large cages are separated by 14 cm^{-1}, which is in agreement with a splitting of approximately 10 cm^{-1} seen in the Raman spectra [22, 23]. Figure 3 also shows that the stretching modes of methane gas are coincident with molecules located in large cages.

Dichlorofluoroethane Hydrates

Figure 4 provides a graphical comparison of the electron density derived from DFT cluster calculations of R141b hydrate, and clearly shows significant overlap of the organic molecule with the water molecules of the small cage leading to this destabilization. Electron density derived for the large cage model shows the guest molecule electron density distinct from that associated with the water molecules, which exhibit several pairs of prominent hydrogen bonds within the plane of the electron density map. Finally, we compare the hydrate forming abilities of 1 and 2 by calculating the largest "molecular diameter" from the DFT electron density of each molecule. Following the method of Hout and Hehre [24], a surface contour of 0.002 $e \cdot Å^3$ was used, which corresponds to van der Waals radii. The calculated molecular diameters were 6.8 Å for 1,1-dichloro-1-fluoroethane and 7.4 Å for the 1,2-dichloro isomer. Using the estimate of 6.6 Å as the "free diameter" inside a large cage of structure II hydrate [25], it is apparent that the 1,2-dichloro isomer is too large to fit inside the large cage of a structure II hydrate.

Classical molecular dynamics simulations of the sII hydrates were performed in the NVT ensemble at 265 K, the highest temperature at which the hydrate structure is maintained in the simulations. When the 1,2-dichloro isomer system is simulated with mobile water molecules at 265 K, the hydrate structure dissociates into aqueous and organic phases. Only at much lower temperatures is the isomer hydrate stable. As discussed previously, our calculated molecular diameters for these guest molecules suggest that size effects should be considered when predicting the ability of these isomers to form hydrates.

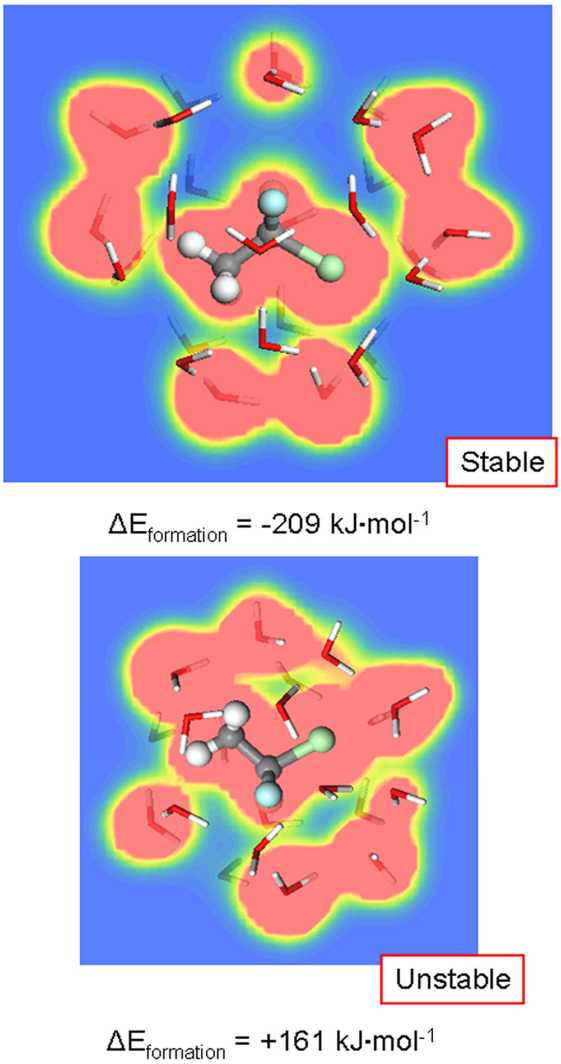

Figure 4 Optimized clusters derived from DFT quantum calculations for the large water cage (top) and the small water cage (bottom) of R141b hydrate. The color maps represent the electron density, and indicate the presence of destabilizing interactions between coordinating water molecules and the guest in the small cage (bottom). Reprinted with permission from ref. 14. Copyright 2007 American Chemical Society.

We also attempted to quantify the rotational motion of dichlorofluoroethane molecules within the water cages. First, we examined the time-dependence of the mean-square-displacement (MSD) for both Cl and F atoms in an attempt to see a difference in atomic diffusivity between the isomers. For both isomers, the MSD values reached plateaus after 5.0 ps (data not shown), which is characteristic of solids and not gases or liquids. The plateau value for Cl and F atoms in R141b hydrate (6.3 Å^2) and the isomer (7.4 Å^2) mirrors the difference in van der Waals diameter of the two molecules, which reinforces the concept that the isomer requires a larger volume than is available in a structure II hydrate (Figure 4).

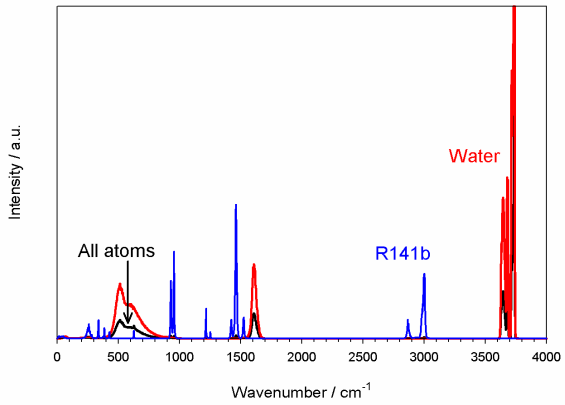

Figure 5 Simulated power spectrum of R141b hydrate (black), showing contributions from water atoms (red) and R141b atoms (blue). Intensities of the R14b peaks were scaled to enhance visibility. Reprinted with permission from ref. 14. Copyright 2007 American Chemical Society.

The vibrational power spectrum of R141b hydrate obtained from the classical molecular dynamics simulations is shown in Figure 5. The overall spectrum is dominated by contributions from water molecules, but peaks due to R141b are visible after rescaling their intensities. The water modes can be classified as follows: O–H stretch (3600 cm^{-1} – 3750 cm^{-1}), H–O–H bend (1500 cm^{-1} – 1700 cm^{-1}), and librations (400 cm^{-1} – 1000 cm^{-1}). Similarly, for R141b, the modes are: C–H stretch (2850 cm^{-1} – 3050 cm^{-1}), C–F stretch and CH_3 bend (1400 cm^{-1} – 1550 cm^{-1}), and C–C stretch (1200 cm^{-1} – 1300 cm^{-1}). Several modes between 600 cm^{-1} and 1530 cm^{-1} involve both Cl and F atoms, and the mode at 630 cm^{-1} is primarily a symmetric carbon-halogen stretch.

The spectrum due to water molecules in R141b hydrate is very similar to that of hexagonal ice (Figure 6). However, for both the high- and low-frequency modes, the ice spectrum shows a more detailed structure. The water peaks are in relatively good agreement with the Raman peaks of hexagonal ice at –4 °C (3150 cm^{-1} – 3375 cm^{-1}, 1640 cm^{-1}, and 600 cm^{-1} – 870 cm^{-1}) [26]. The increased rotational motion of water molecules in the hydrate phase compared to hexagonal ice may explain the difference in fine structure between 3600 cm^{-1} and 3750 cm^{-1}.

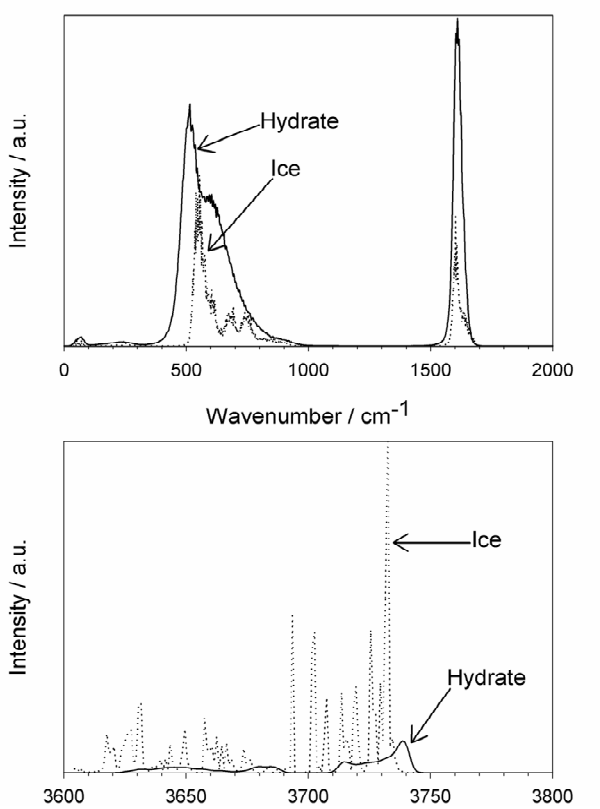

Figure 6 Comparison of power spectra (H atoms only) of R141b hydrate (solid line) with hexagonal ice (dotted line). The intensities at lower frequencies (top) have been amplified for ease of viewing. Reprinted with permission from ref. 14. Copyright 2007 American Chemical Society.

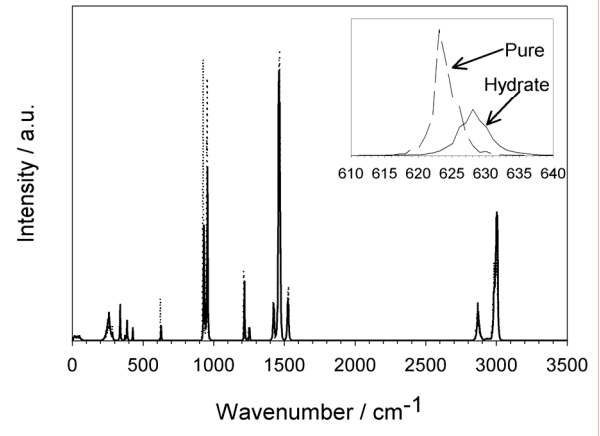

Figure 7 Simulated power spectrum of R141b in both the hydrate (solid line) and (pure) gas phases (dashed line). The inset shows the peak shift at 628 cm^{-1}. Reprinted with permission from ref. 14. Copyright 2007 American Chemical Society.

A comparison of the R141b hydrate power spectrum with that of pure R141b is shown in Figure 7. For all bending and stretching modes that involve C–Cl or C–F bonds, hydrate peaks were shifted by 5 cm^{-1} to 10 cm^{-1} higher than those in pure R141b. Modes involving C–H bonds occur at identical frequencies in the two phases. No peak shifts were seen in the librational modes (< 500 cm^{-1}), which indicate that the nonbonding environment experienced by R141b in the two phases is similar. Despite the presence of hydrogen bonds between halogen atoms and water molecules, the overall hydrophobic effect of R141b surrounded by water molecules is a strengthening of intramolecular interactions (blue shift in bonded modes) with no change in intermolecular interactions.

ACKNOWLEDGEMENTS

We acknowledge support from the Sandia National Laboratories under its LDRD program. Sandia is a multiprogram laboratory operated by Sandia Corporation, a Lockheed Martin Company, for the United States Department of Energy's National Nuclear Security Administration under contract DE-AC04-94AL85000.

REFERENCES

[1] Forrisddahl OK, Kvamme B, Haymet ADJ. *Methane clathrate hydrates: Melting, supercooling and phase separation from molecular dynamics computer simulations*. Molecular Physics 1996;89(3):819-834.

[2] Alavi S, Ripmeester JA, Klug DD. *Molecular-dynamics study of structure II hydrogen clathrates*. Journal of Chemical Physics 2005;123(2):024507.

[3] English NJ, MacElroy JMD. *Structural and dynamical properties of methane clathrate hydrates*. Journal of Computational Chemistry 2003;24(13):1569-1581.

[4] Moon C, Taylor PC, Rodger PM. *Molecular dynamics study of gas hydrate formation.* Journal of the American Chemical Society 2003;125(16):4706-4707.

[5] Storr MT, Taylor PC, Monfort JP, Rodger PM. *Kinetic inhibitor of hydrate crystallization*. Journal of the American Chemical Society 2004;126(5):1569-1576.

[6] Chialvo AA, Houssa M, Cummings PT. *Molecular dynamics study of the structure and thermophysical properties of model sI clathrate hydrates*. Journal of Physical Chemistry B 2002;106(2):442-451.

[7] Cao ZT, Tester JW, Sparks KA, Trout BL. *Molecular computations using robust*

hydrocarbon-water potentials for predicting gas hydrate phase equilibria. Journal of Physical Chemistry B 2001;105(44):10950-10960.
[8] Zele SR, Lee S-Y, Holder GD. *A theory of lattice distortion in gas hydrates*. Journal of Physical Chemistry B 1999;103(46):10250-10257.
[9] Klauda JB, Sandler SI. *Phase behavior of clathrate hydrates: A model for single and multiple gas component hydrates*. Chemical Engineering Science 2003;58(1):27-41.
[10] Klauda JB, Sandler SI. *Ab initio intermolecular potentials for gas hydrates and their predictions*. Journal of Physical Chemistry B 2002;106(22):5722-5732.
[11] Frenkel D, Smit B. *Understanding molecular simulation: From algorithms to applications*. 2nd ed.; San Diego: Academic Press, 2002.
[12] Dauber-Osguthorpe P, Roberts VA, Osguthorpe DJ, Wolff J, Genest M, Hagler AT. *Structure and energetics of ligand binding to proteins: Escherichia coli dihydrofolate reductase-trimethoprim, a drug-receptor system.* Proteins: Structure, Function, and Genetics 1988;4(1):31-47.
[13] Greathouse JA, Cygan RT, Simmons BA. *Vibrational spectra of methane clathrate hydrates from molecular dynamics simulation*. Journal of Physical Chemistry B 2006;110(13):6428-6431.
[14] Greathouse JA, Cygan RT, Bradshaw RW, Majzoub EH, Simmons BA. *Computational and spectroscopic studies of dichlorofluoroethane hydrate structure and stability*. Journal of Physical Chemistry C 2007;111(45):16787-16795.
[15] McMullan RK, Kvick A. *Neutron diffraction study of the structure II clathrate hydrate: 3.5Xe.8CCl_4.136D_2O at 13 and 100 K*. Acta Crystallographica Section B-Structural Science 1990;46:390-399.
[16] Hollander F, Jeffrey GA. *Neutron diffraction study of the crystal structure of ethylene oxide deuterohydrate at 80 K*. Journal of Chemical Physics 1977;66(10):4699-4705.
[17] Delley B. *An all-electron numerical-method for solving the local density functional for polyatomic-molecules*. Journal of Chemical Physics 1990;92(1):508-517.
[18] Delley B. *From molecules to solids with the DMol(3) approach*. Journal of Chemical Physics 2000;113(18):7756-7764.
[19] Wilson EB, Cross PC, Decius JC. *Molecular vibrations: The theory of infrared and Raman vibrational spectra*. New York: Courier Dover, 1980.
[20] Gutt G, Asmussen B, Press W, Johnson MR, Handa YP, Tse JS. *The structure of deuterated methane-hydrate*. Journal of Chemical Physics 2000;113(111):4713-4721.
[21] Davidson DW, Handa YP, Ratcliffe CI, Tse JS, Powell BM. *The ability of small molecules to form clathrate hydrates of structure II*. Nature 1984;311:142-143.
[22] Sum AK, Burruss RC, Sloan ED. *Measurement of clathrate hydrates via Raman spectroscopy*. Journal of Physical Chemistry B 1997;101(38):7371-7377.
[23] Uchida T, Hirano T, Ebinuma T, Narita H, Gohara K, Mae S, Matsumoto R. *Raman spectroscopic determination of hydration number of methane hydrates*. AIChE Journal 1999;45(12):2641-2645.
[24] Hout RF, Hehre WJ. *Atomic fits to electron densities in polyatomic molecules. Correlation of atom size and charge*. Journal of the American Chemical Society 1983;105:3728-3729.
[25] Davidson DW: *Clathrate hydrates* In: Water: A comprehensive treatise, volume 2. F. Franks, (Ed.) New York: Plenum Press, 1973; p 130.
[26] Scherer JR, Snyder RG. *Raman intensities of single-crystal ice Ih*. Journal of Chemical Physics 1977;67(11):4794-4811.